



On the Rotation Curve of Disk Galaxies in General Relativity

Luca Ciotti

Department of Physics and Astronomy “Augusto Righi”, University of Bologna, via Gobetti 93/2, I-40129 Bologna, Italy

Received 2022 June 17; revised 2022 July 18; accepted 2022 July 18; published 2022 September 13

Abstract

Recently, it has been suggested that the phenomenology of flat rotation curves observed at large radii in the equatorial plane of disk galaxies can be explained as a manifestation of general relativity (GR) instead of the effect of dark matter (DM) halos. In this paper, by using the well-known weak-field, low-velocity gravitomagnetic formulation of GR, the expected rotation curves in GR are rigorously obtained for purely baryonic disk models with realistic density profiles and compared with the predictions of Newtonian gravity for the same disks in absence of DM. As expected, the resulting rotation curves are indistinguishable, with GR corrections at all radii of the order $v^2/c^2 \approx 10^{-6}$. Next, the gravitomagnetic Jeans equations for two-integral stellar systems are derived, and then solved for the Miyamoto–Nagai disk model, showing that finite-thickness effects do not change the previous conclusions. Therefore, the observed phenomenology of galactic rotation curves at large radii requires DM in GR exactly as in Newtonian gravity, unless the cases here explored are reconsidered in the full GR framework with substantially different results (with the surprising consequence that the weak-field approximation of GR cannot be applied to the study of rotating systems in the weak-field regime). In this article, the mathematical framework is described in detail, so that the present study can be extended to other disk models, or to elliptical galaxies (where DM is also required in Newtonian gravity, but their rotational support can be much less than in disk galaxies).

Unified Astronomy Thesaurus concepts: [Galaxy dark matter halos \(1880\)](#); [Galaxy rotation curves \(619\)](#); [General relativity \(641\)](#)

1. Introduction

Recently, following the original suggestion of Cooperstock and Tieu (2007; see also Balasin & Grumiller 2008), several papers have addressed the interesting possibility that the observed phenomenology of rotation curves in disk galaxies can be explained by general relativity effects (hereafter, GR) peculiar to rotating systems, without the need to invoke the presence of dark matter (hereafter, DM) halos in order to produce the flat behavior at large galactocentric distances.

Unfortunately, no definite consensus about the importance of GR effects on the rotation curves of disk galaxies has seemed to be reached, with widely different conclusions ranging from support to the hypothesis to the identification of possible mathematical issues affecting the disk models used to compute the GR solutions (for a representative, but almost certainly incomplete list of papers representing the different positions, see, e.g., Vogt & Letelier 2005a, 2005b; Korzynski 2005; Cross 2006; Fuchs & Phleps 2006; Carrick & Cooperstock 2012; Rowland 2015; Deledicque 2019; Crosta et al. 2020; Ludwig 2021; Ruggiero et al. 2021; Toth 2021; Astesiano & Ruggiero 2022; Ludwig 2022, and references therein).

If confirmed, the suggestion above would be a most surprising result, with consequences extending well beyond the problem of the interpretation of galaxy rotation curves, and perhaps even beyond the problem of the existence of DM. A list of some of these consequences (not necessarily in order of importance) is the following. (1) Usually, it is expected that lowest-order corrections of GR to Newtonian dynamics are of the order v^2/c^2 , where v is a characteristic velocity associated with the Newtonian gravitational potential of the system, and c

is the speed of light. In astronomical systems where the presence of DM is required by Newtonian gravity, $v/c \approx 10^{-3}$ or less; therefore such systems are *empirically* in the GR weak-field regime. If the flat region of rotation curves is a GR effect, then we face the problem of explaining in physical terms how an expected effect of the order $\approx 10^{-6}$ actually becomes more important than the zeroth-order Newtonian term: we notice that mathematically such a behavior characterizes singular perturbation theory. (2) In case the previous point is satisfactorily answered, we should then explain why other effects of GR in the weak-field approximation (not directly related to rotation) remain at the level of small perturbations, for example *by requiring* the presence of DM in order to reproduce gravitational lensing, and correctly predicting the small amount of planetary precession left unexplained once Newtonian precession is considered.¹ (3) DM is clearly required by Newtonian gravity not only in rotating disk galaxies, but also in velocity dispersion (pressure) supported astronomical systems with *low* ordered rotation, such as elliptical galaxies and clusters of galaxies (with converging predictions about the structural properties of the inferred DM halos obtained from different diagnostics, such as dynamical analysis, the modeling of X-ray-emitting halos, and gravitational lensing; see, e.g., BT08, Bertin 2014).

Different strategies can be imagined to test the possibility of a general relativistic origin of the flat rotation curve in disk galaxies.

¹ Unfortunately, in too simplistic descriptions it is said that GR “explains the precession of Mercury’s perihelion,” conveying the wrong impression of a major effect, instead of a small (but physically dramatic) correction. In Newtonian gravity the perihelion of Mercury’s orbit is predicted to precess ≈ 531 arcseconds/century due to planetary perturbations, against the observed ≈ 574 arcseconds/century (e.g., Fitzpatrick 2012), while GR accounts for the remaining ≈ 43 arcseconds/century. The explanation of the precession of Mercury’s perihelion is a triumph both of GR *and* of Newtonian theory, the latter not least for the bold statement that the small discrepancy of ≈ 43 arcseconds/century cannot be accounted for in its framework.



In the first, one can just try to reproduce the expected GR rotation curve of some specific galaxy starting from its observed baryonic (e.g., stars and gas) density profile. This attempt suffers from some shortcomings. In fact, the mathematical modeling in GR (also considering effects such as sparse data points, error bars, and so on) is more complicated than in Newtonian gravity, and great care is needed to interpret the results. Moreover, it should be recalled that the Newtonian rotation curve of a purely baryonic razor-thin exponential disk (the common stellar density profile observed in disk galaxies) of total mass M_d and scale length R_d , is *not* Keplerian over a large fraction of the stellar disk (see, e.g., Binney & Tremaine 2008 and Ciotti 2021, hereafter BT08 and C21, respectively), increasing from the center, reaching a quite shallow maximum at $\approx 2 R_d$, and remaining almost flat up to $\approx 3 R_d$ (a radius already encircling $\approx 0.8 M_d$; see Section 4.1). It follows that in Newtonian gravity observed *stellar* rotation curves in disk galaxies hardly require any DM over a large fraction of the optical disk, while DM is certainly required by the rotation curves at larger galactocentric distances measured by radio observations in H I gas (see, e.g., Kalnajs 1983; van Albada et al. 1985; Kent 1986; van Albada & Sancisi 1986, and, in particular, Chapter 20 in Bertin 2014 for a complete account of the situation), and theoretically by stability arguments (Ostriker & Peebles 1973). Therefore, in this first approach the prediction of a GR rotation curve *not* declining with R over a large part of the *stellar* disk would just be what was expected in case of small GR corrections to the Newtonian rotation curve.

In a second approach (that we follow in this paper), one avoids direct comparison with observational data but instead constructs the Newtonian and the (weak-field) GR rotation curves produced in the equatorial plane by a rotating stellar disk without DM, with total baryonic mass, scale length, and density profile similar to those observed in real disks/elliptical galaxies. The obvious advantage of this approach is that, whatever the solution is, we learn something. In fact, let us assume that the obtained rotation curve in GR and in Newtonian gravity are essentially the same (the common expectation): after excluding the case of mathematical/physical errors in the modeling, only three conclusions are possible. Conclusion 1: if we still pretend that GR can explain the flat profile of the rotation curves of disk galaxies at large radii without invoking the presence of DM halos, then we must conclude that the adopted weak-field approximation of GR cannot be used to describe the dynamics of disk galaxies, even though these systems *are* (empirically) in the weak-field regime. Conclusion 2: the weak-field approximation of GR can be used to describe the weak-field regime of disk galaxies, but in the explored cases we fail to reproduce the flat region of rotation curves at large radii (i.e., well beyond the geometrical outskirts of the optical stellar disk) because we assumed a too simple/idealized orbital structure for the stars producing the velocity-dependent component of the GR force in the equatorial plane. Conclusion 3: the weak-field approximation can be used to describe the weak-field regime in disk galaxies, and DM halos are required in GR as they are in Newtonian gravity.

Conclusion 1 would be quite formidable, and should be proved convincingly showing that higher-order effects not considered in the weak-field expansion used are even more important than those considered or, better, by presenting a case obtained by numerically solving the full (nonlinear) GR equations for a realistic baryonic disk in the weak-field regime, with a predicted rotation curve significantly different with respect to the Newtonian rotation curve for the same baryonic

disk, i.e., with GR “corrections” well above 300% and increasing as the square root of the galactocentric radius at larger and larger distances from the center. Conclusion 2 would imply that a universal property of the rotation curves of disk galaxies is a GR effect produced by peculiar (in actual fact, never observed) significant streaming motions of the stellar populations along the vertical and radial directions (see Section 4 for details). As we will see, even if with the aid of simple models (however, the most realistic used so far in this problem), in this paper we present quite strong evidence that a commonly adopted weak-field approximation of GR predicts rotation curves indistinguishable from the Newtonian ones in absence of DM, therefore strongly supporting Conclusion 3 above. In order to illustrate the results in the most transparent way, the mathematical setting is rigorously presented, and all the assumptions made explicitly stated, so that an interested reader is in a position to repeat and extend the study. We use cylindrical coordinates (R, φ, z) , and vectors are in boldface.

The paper is organized as follows. In Section 2 we recall the expression for the gravitomagnetic equations in case of low velocities for the sources, and the equations of motion for a low-velocity test mass, together with the general integral expressions of the gravitomagnetic fields in terms of the mass current for axisymmetric systems, in the two alternative formulations of elliptic integrals and Bessel functions, also discussing their convergence properties. In Section 3 we consider the case of the rotation curve of generic razor-thin disks supported by circular orbits, and provide a regular series expansion of the rotational velocity in terms of the small expansion parameter $\epsilon = v_0^2/c^2$ (the square of the ratio between a characteristic Newtonian velocity of the disk and the speed of light c). In Section 4 we consider the explicit case of a baryonic exponential disk, and we obtain essentially identical Newtonian and GR rotation curves. The result is then confirmed with the aid of a Kuzmin disk, where the first-order GR correction can be computed analytically. In Section 5, we relax the assumption of razor-thin disks, and we derive the gravitomagnetic Jeans equations for collisionless axisymmetric systems supported by a two-integral phase-space distribution function. This allows to investigate finite-thickness GR effects on the rotational velocity in the equatorial plane. The case of the Miyamoto–Nagai disk is studied, again fully confirming the results for razor-thin disks. Section 6 concludes, while in the Appendix mathematical details are provided.

2. The Gravitomagnetic Equations

In this paper, following previous works, we adopt the gravitomagnetic formulation of GR in the weak-field limit, for low velocities and for steady motions of the sources of the gravitational field, where the equations, truncated at the first order (inclusive) of the source velocity in unit of the speed of light c , reduce to

$$\begin{cases} \nabla \cdot \mathbf{E} = -4\pi G\rho(\mathbf{x}), & \nabla \wedge \mathbf{E} = 0, \\ \nabla \cdot \mathbf{B} = 0, & \nabla \wedge \mathbf{B} = \frac{16\pi G}{c^2} \mathbf{j}(\mathbf{x}), \end{cases} \quad (1)$$

(see, e.g., Landau & Lifshitz 1971 and Poisson & Will 2014, for a detailed description of higher-order post-Newtonian expansions; see also Rindler 1997; Lynden-Bell & Nouri-Zonoz 1998; Mashhoon et al. 1999; Clark & Tucker 2000; Ruggiero & Tartaglia 2002; Mashhoon 2008; Costa & Natário 2021, and

Ruggiero 2021). We indicate with \wedge the vector (cross) product, ∇ is the usual nabla operator, and $\mathbf{j} = \rho\mathbf{v}$ is the gravitational current density, ρ and \mathbf{v} being the mass density and velocity field of the sources. Notice that at this expansion order the gravitoelectric field $\mathbf{E} = -\nabla\phi$ is just the Newtonian field produced by ρ , so that in Equation (1) the GR effects arise only from the gravitomagnetic Ampère’s law. The equation of motion of a test star at position \mathbf{x}_* is given analogously by the low-velocity limit of the Lorentz force (e.g., see Feynman et al. 1977; Jackson 1998, hereafter J98),

$$\frac{d^2\mathbf{x}_*}{dt^2} = \mathbf{E}(\mathbf{x}_*) - \mathbf{v}_* \wedge \mathbf{B}(\mathbf{x}_*), \quad \mathbf{v}_* = \frac{d\mathbf{x}_*}{dt}, \quad (2)$$

where $\mathbf{B}(\mathbf{x}_*)$ is the gravitomagnetic field produced at \mathbf{x}_* by the total gravitational current density distribution: notice the minus sign in front of the gravitomagnetic force, instead of the plus sign appearing in the electromagnetic case. For future use (see Section 4) it is useful to distinguish between the velocity \mathbf{v}_* of the test star, and the velocity $\mathbf{v}(\mathbf{x}_*)$ of the mass current of the sources at \mathbf{x}_* , even though we anticipate that in the case of razor-thin disks made by circular orbits (see Section 3), necessarily $\mathbf{v}_* = \mathbf{v}(\mathbf{x}_*)$.

Equations (1) are formally coincident with the (stationary) Maxwell equations, so the mathematical treatment is the same as in electrodynamics; however, due to some mathematical subtlety in the present astronomical problem, it is useful to list the most important properties of the field \mathbf{B} in the general case. As is well known (e.g., see J98), for a current density \mathbf{j} well behaved at infinity,

$$\begin{aligned} \mathbf{B}(\mathbf{x}) &= \frac{4G}{c^2} \int \frac{\mathbf{j}(\mathbf{y}) \wedge (\mathbf{x} - \mathbf{y})}{\|\mathbf{x} - \mathbf{y}\|^3} d^3\mathbf{y} = \nabla \wedge \mathbf{A}(\mathbf{x}), \\ \mathbf{A}(\mathbf{x}) &= \frac{4G}{c^2} \int \frac{\mathbf{j}(\mathbf{y})}{\|\mathbf{x} - \mathbf{y}\|} d^3\mathbf{y}, \end{aligned} \quad (3)$$

where the first expression is the Biot–Savart law, $\|\dots\|$ is the standard Euclidean norm, and \mathbf{A} is the gravitomagnetic potential vector in the Coulomb gauge, particularly appropriate for the magnetostatic case of steady currents. The Biot–Savart law can be proved by carrying the ∇ operator acting on \mathbf{x} (hereafter ∇_x) under the integral sign in the second expression above, and then using the general identity $\nabla_x \wedge (\mathbf{f}g) = g \nabla_x \wedge \mathbf{f} + (\nabla_x g) \wedge \mathbf{f}$, where in the present case the meaning of the functions $g(\mathbf{x}, \mathbf{y})$ and $\mathbf{f}(\mathbf{y})$ is obvious, and so $\nabla_x \wedge (\mathbf{f}g) = (\nabla_x g) \wedge \mathbf{f}$. A useful (and less known) equivalent expression of the Biot–Savart law can be obtained from the last identity by recognizing that $\nabla_x \|\mathbf{x} - \mathbf{y}\| = -\nabla_y \|\mathbf{x} - \mathbf{y}\|$, so that we have $\nabla_x \wedge (\mathbf{f}g) = -(\nabla_y g) \wedge \mathbf{f} = g \nabla_y \wedge \mathbf{f} - \nabla_y \wedge (\mathbf{f}g)$, where the last expression follows from the identity $\nabla_y \wedge (\mathbf{f}g) = g \nabla_y \wedge \mathbf{f} + (\nabla_y g) \wedge \mathbf{f}$. As the volume integral of $\nabla_y \wedge (\mathbf{f}g)$ vanishes for well-behaved fields at infinity, we finally obtain the alternative expression

$$\mathbf{B}(\mathbf{x}) = \frac{4G}{c^2} \int \frac{\nabla_y \wedge \mathbf{j}(\mathbf{y})}{\|\mathbf{x} - \mathbf{y}\|} d^3\mathbf{y}, \quad (4)$$

which we will use later on. Before addressing our specific problem, it is important to recall some convergence property of the fields \mathbf{A} and \mathbf{B} : notice that the only troublesome points \mathbf{x} are those inside the current distribution, when the denominators in the

integrands vanish for $\mathbf{y} = \mathbf{x}$. The following results can easily be established.

(1) For well-behaved, genuinely three-dimensional currents, the integrals in Equation (3) converge absolutely, i.e., the volume integral of the norm of the integrand converges, as can be seen by changing variable $\mathbf{y} = \mathbf{r} + \mathbf{x}$ at fixed \mathbf{x} , and using spherical coordinates for \mathbf{r} . It follows that each component of the \mathbf{A} and \mathbf{B} fields is also absolutely convergent. The Fubini–Tonelli theorem then assures that the integrals can be evaluated as repeated integrals, and that the order of integration does not matter, even though integrable singularities over sets of null measure can appear: from the physical point of view such singularities have no consequences, but attention should be paid in numerical studies.

(2) For well-behaved, razor-thin currents in the $z = 0$ plane,

$$\mathbf{j}(\mathbf{y}) = \chi(y_1, y_2) \delta(y_3), \quad \chi = (\chi_1, \chi_2, 0), \quad (5)$$

where δ is the Dirac delta function and χ is the surface current density, the \mathbf{A} and \mathbf{B} integrals in Equation (3) again converge absolutely for all points \mathbf{x} outside the current plane, and \mathbf{A} also for points in the $z = 0$ plane, as can be proved with the change of variables $\mathbf{y} = \mathbf{r} + \mathbf{x}$, and expressing \mathbf{r} in cylindrical coordinates. The absolute convergence of \mathbf{B} in the $z = 0$ plane cannot instead be established just from boundedness of $\|\chi\|$, as the corresponding integral in Equation (3) diverges logarithmically for $\|\mathbf{r}\| \rightarrow 0$. However, from specialization of Equation (4) to razor-thin currents,

$$\begin{aligned} \mathbf{B}(\mathbf{x}) &= \frac{4G}{c^2} \int \frac{\nabla_y \wedge \chi(\mathbf{y})}{\|\mathbf{x} - \mathbf{y}\|} \delta(y_3) d^3\mathbf{y} \\ &+ \frac{4G}{c^2} \mathbf{e}_z \wedge \int \frac{\chi(\mathbf{y})}{\|\mathbf{x} - \mathbf{y}\|} \delta'(y_3) d^3\mathbf{y}, \end{aligned} \quad (6)$$

where $\mathbf{e}_z = (0, 0, 1)$, and proceeding as in point (2), it follows that absolute convergence of \mathbf{B} for points in the disk (where the second integral above vanishes from well-known properties of δ' , and the fact that χ is independent of y_3) is guaranteed under the additional request that $\|\nabla_y \wedge \chi\|$ is well behaved, a condition obeyed by the disks considered in this paper.

(3) Finally, for razor-thin currents, Equations (3)–(4) show that $A_3 = 0$ everywhere, and $B_1 = B_2 = 0$ for points in the current plane.

In summary, the general results above assure that not only for three-dimensional currents but also for points inside razor-thin disks, the gravitomagnetic field cannot develop nasty singularities if the surface density of the disk is sufficiently well behaved, and \mathbf{B} and \mathbf{A} are given by absolutely converging integrals.

2.1. The Axisymmetric Case

We now restrict to the case of axisymmetric systems, the subject of this paper. In cylindrical coordinates $\mathbf{x} = R\mathbf{e}_R + z\mathbf{e}_z$, where $\mathbf{e}_R = (\cos \varphi, \sin \varphi, 0)$ and $\mathbf{e}_z = (0, 0, 1)$, so that $\rho = \rho(R, z)$; we will not discuss how to obtain the associated Newtonian gravitational potential $\phi(R, z)$, a problem fully addressed in the literature (see, e.g., BT08; C21). For the moment, purely circular orbits are considered for the sources, with a velocity field $\mathbf{v} = v(R, z)\mathbf{e}_\varphi$, where $\mathbf{e}_\varphi = (-\cos \varphi, \sin \varphi, 0)$, so that

$$\mathbf{j} = j(R, z)\mathbf{e}_\varphi, \quad j = \rho(R, z)v(R, z). \quad (7)$$

The condition of circular orbits will be relaxed in Section 4; however, notice that this is a quite natural idealization when considering the rotation curve produced by razor-thin disks in

their equatorial plane (see Section 3). Obviously, in a three-dimensional system, a purely circular current field outside the equatorial plane requires a vertical pressure gradient (or a vertical velocity dispersion field, as is the case in Section 4).

In order to evaluate the integrals in Equation (3), we introduce the source coordinates $\mathbf{y} = \xi \mathbf{e}_{R'} + z' \mathbf{e}_z$, with $\mathbf{e}_{R'} = (\cos \varphi', \sin \varphi', 0)$ and $\mathbf{e}_{\varphi'} = (-\cos \varphi', \sin \varphi', 0)$. It is a simple exercise to show that for axisymmetric currents the fields \mathbf{B} and \mathbf{A} are rotationally invariant (i.e., independent of φ), so that they can be evaluated without loss of generality at $\varphi = 0$, where $\mathbf{x} = (R, 0, z)$. For the potential vector \mathbf{A} , it is trivial to prove that for sufficiently regular currents (also in the razor-thin case), not only $A_z = \mathbf{A} \cdot \mathbf{e}_z = 0$ everywhere, in accordance with Point (3) above, but also $A_R = \mathbf{A} \cdot \mathbf{e}_R = 0$ everywhere, while the only nonzero component is

$$\begin{aligned} A_\varphi(R, z) &= \mathbf{A} \cdot \mathbf{e}_\varphi \\ &= \frac{4G}{c^2} \int \frac{j(\xi, z') \cos \varphi'}{(R^2 + \xi^2 - 2R\xi \cos \varphi' + \Delta z^2)^{1/2}} d^3\mathbf{y}, \\ \Delta z &= z - z', \end{aligned} \quad (8)$$

where $d^3\mathbf{y} = \xi d\xi d\varphi' dz'$.

An analogous treatment of the \mathbf{B} field in Equation (3) shows quite easily that $B_\varphi = \mathbf{B} \cdot \mathbf{e}_\varphi = 0$ everywhere,² while

$$\begin{cases} B_R(R, z) = \mathbf{B} \cdot \mathbf{e}_R = \frac{4G}{c^2} \int \frac{j(\xi, z') \Delta z \cos \varphi'}{(R^2 + \xi^2 - 2R\xi \cos \varphi' + \Delta z^2)^{3/2}} d^3\mathbf{y}, \\ B_z(R, z) = \mathbf{B} \cdot \mathbf{e}_z = \frac{4G}{c^2} \int \frac{j(\xi, z') (\xi - R \cos \varphi')}{(R^2 + \xi^2 - 2R\xi \cos \varphi' + \Delta z^2)^{3/2}} d^3\mathbf{y}; \end{cases} \quad (9)$$

therefore, $B_R(R, 0) = 0$ for currents with reflection symmetry about the equatorial plane, $j(R, z) = j(R, -z)$, and in particular for razor-thin currents, again in accordance with Point (3) above. Notice that from Equation (A1) it follows that for the axisymmetric currents in Equation (7):

$$\nabla \wedge \mathbf{A} = -\frac{\partial A_\varphi}{\partial z} \mathbf{e}_R + \frac{1}{R} \frac{\partial R A_\varphi}{\partial R} \mathbf{e}_z. \quad (10)$$

As a sanity check, it is possible to verify by direct evaluation that Equations (8)–(10) are in fact equivalent to Equation (9). Notice also that Equation (10) can be applied analogously to the current in Equation (7), to compute the numerator of the integrand in the alternative formulation of the Biot–Savart law in Equation (4).

² The only delicate point is the vanishing of B_φ over the singular ring $\xi = R$ and $\Delta z = 0$ inside the current. This can be proved considering $\Delta z = 0$ and $\xi \rightarrow R$, or $\xi = R$ and $\Delta z \rightarrow 0$ in the integral over φ' .

In summary, the gravitomagnetic fields in the plane $z = 0$, produced by the axisymmetric currents in Equation (7) with reflection symmetry plane $z = 0$ (and in particular in the razor-thin case), can be written in full generality as $\mathbf{A} = A_\varphi(R) \mathbf{e}_\varphi$ and $\mathbf{B} = B_z(R) \mathbf{e}_z$, where the functions $A_\varphi(R)$ and $B_z(R)$ are obtained from Equations (8)–(9) setting $z = 0$.

2.2. The Field in Terms of Complete Elliptic Integrals

In potential theory it is customary to integrate Equations (8)–(9) first on φ' , as the knowledge of the specific form of $j(R, z)$ is not required. From the general results mentioned in Points (1) and (2) after Equation (4), the Fubini–Tonelli theorem assures that this is legitimate, and, at worst, only integrable singularities over zero-measure sets occur. In fact, from Equations (8) and (A5),

$$A_\varphi(R, z) = \frac{4G}{c^2} \int_0^\infty \xi d\xi \int_{-\infty}^\infty j(\xi, z') \mathcal{F}_1 dz', \quad (11)$$

where the function $\mathcal{F}_1(R, \xi, \Delta z)$ can be expressed in terms of complete elliptic integrals of first and second kind, $\mathbf{K}(k)$ and $\mathbf{E}(k)$, and k is given in Equation (A6). Notice that, according to Equation (A8), \mathcal{F}_1 presents an integrable singularity for $k = 1$, i.e., over the ring $\xi = R$ at $z' = z$, of easy treatment in numerical applications.

The components of the \mathbf{B} field can be obtained from differentiation of $A_\varphi(R, z)$ by using Equations (10), (11), and (A3); however, when using the formulation in terms of complete elliptic integrals, it is convenient to avoid explicit differentiation, and instead work with the Biot–Savart law in Equation (9), integrating first over φ' , and then proceeding as follows. For the radial component, B_R , the resulting kernel in the integrand is a perfect differential of \mathcal{F}_1 with respect to both z or z' : the first possibility just corresponds to evaluate $-\partial A_\varphi / \partial z$ as required by Equation (10). In the second option one avoids differentiation of the elliptic integrals, performing integration by parts with respect to z' (provided the current j is well behaved for $|z'| \rightarrow \infty$, the usual situation), and noticing that $\partial \mathcal{F}_1 / \partial z = -\partial \mathcal{F}_1 / \partial z'$. For the vertical component, B_z , we also recognize the kernel as an exact differential with respect to ξ of \mathcal{F}_0 in Equation (A4), and again we can avoid differentiation of the elliptic integrals integrating by parts (provided j is well behaved for $\xi \rightarrow \infty$). One finally obtains

$$\begin{cases} B_R(R, z) = \frac{4G}{c^2} \int_0^\infty \xi d\xi \int_{-\infty}^\infty j(\xi, z') \frac{\partial \mathcal{F}_1}{\partial z'} dz' = -\frac{4G}{c^2} \int_0^\infty \xi d\xi \int_{-\infty}^\infty \frac{\partial j(\xi, z')}{\partial z'} \mathcal{F}_1 dz', \\ B_z(R, z) = -\frac{4G}{c^2} \int_{-\infty}^\infty dz' \int_0^\infty \xi j(\xi, z') \frac{\partial \mathcal{F}_0}{\partial \xi} d\xi = \frac{4G}{c^2} \int_{-\infty}^\infty dz' \int_0^\infty \frac{\partial \xi j(\xi, z')}{\partial \xi} \mathcal{F}_0 d\xi \end{cases} \quad (12)$$

Notice that the first expression for B_z can be also obtained from Equation (10), by using the nontrivial identity (A7). Of course, the two second identities above are not unexpected: they are just how the Biot–Savart law in Equation (4) reduces in axisymmetric systems. These expressions are particularly useful when working with regular currents, as the integrable singularity in \mathcal{F}_0 and \mathcal{F}_1 can be explicitly taken into account. In particular, the second expression for B_z not only shows again that the field is well behaved inside a regular razor-thin current, confirming the conclusion in Point (2) above, but also shows that for a surface

density current with an abrupt radial truncation, the field diverges at the edge, in analogy with the well-known feature of the rotation curve produced by truncated disks (e.g., see Casertano 1983; see also exercises 5.4–5.6 in C21).

2.3. The Field in Terms of Bessel Functions

As is well known, the integrals appearing in potential theory can also be expressed in alternative formulations, for example as Fourier–Bessel series, obtained by using the apparatus of Green functions and Hankel transforms (e.g., Toomre 1963; see also J98, BT08, and C21). This approach is very elegant from the analytical point of view, but the numerical implementation is not straightforward, due to the oscillatory nature of Bessel functions and the slow convergence of their integrals. In practice, we substitute Equation (A9) in the second formula of Equation (3) and we perform a first integration over φ' . The current in Equation (7) is a vector quantity, and so in principle two integrals should be performed over the components of $\mathbf{e}_{\varphi'}$; however, it is possible to reduce the computation to a single integration, observing that the two components of $\mathbf{e}_{\varphi'}$ are just the real and imaginary parts of the complex number $ie^{i\varphi'}$. We therefore introduce the complex current $j^* = ie^{i\varphi'}j(\xi, z')$, we determine the complex vector potential \mathbf{A}^* with a Fourier–Bessel expansion, and finally we switch back to the vectorial representation by separating the real and imaginary parts. The integration of j^* over φ' is elementary, and only the $m=1$ component survives, producing $2\pi i\delta_{m1}j(\xi, z')$. Therefore, the final expression is in terms of a Hankel transform of index 1 for the current (see, e.g., J98 for the case of the potential vector of a circular spire). The last step is the evaluation of the real and imaginary parts of the resulting expression, and it can immediately be shown that the result is just proportional to \mathbf{e}_{φ} , i.e., we prove again that the potential vector is just $\mathbf{A} = A_{\varphi}\mathbf{e}_{\varphi}$. In particular,

$$A_{\varphi}(R, z) = \frac{8\pi G}{c^2} \int_0^{\infty} J_1(\lambda R) d\lambda \int_{-\infty}^{\infty} e^{-\lambda|\Delta z|} \hat{j}_1(\lambda, z') dz', \quad (13)$$

where

$$\hat{j}_1(\lambda, z') = \int_0^{\infty} \xi J_1(\lambda\xi) j(\xi, z') d\xi \quad (14)$$

is the Hankel transform of order 1 of the current density: reassuringly, by inverting the order of integration in the triple integral in Equation (13), and performing first the integration over λ , Equation (2.12.38.1) in Prudnikov et al. (1986, hereafter P86) proves that the resulting expression coincides³ with Equation (11).

From Equation (10) we then obtain the two components of the \mathbf{B} field:

$$\begin{cases} B_R(R, z) = \frac{8\pi G}{c^2} \int_0^{\infty} \lambda J_1(\lambda R) d\lambda \int_{-\infty}^{\infty} \text{sign}(\Delta z) e^{-\lambda|\Delta z|} \hat{j}_1(\lambda, z') dz', \\ B_z(R, z) = \frac{8\pi G}{c^2} \int_0^{\infty} \lambda J_0(\lambda R) d\lambda \int_{-\infty}^{\infty} e^{-\lambda|\Delta z|} \hat{j}_1(\lambda, z') dz', \end{cases} \quad (15)$$

³ The equivalence in the special case of $\Delta z = 0$, i.e., for points in the plane of razor-thin currents, can also be proved by using Equation (2.12.31.1) in P86, and Equation (6.576.2) in Gradshteyn et al. (2007, hereafter GR07).

where the expression for B_z derives from the identity $d[xJ_1(x)]/dx = xJ_0(x)$. The proof of equivalence of Equations (12)–(15) is important but quite laborious, and requires some comment. For B_R we move λ in front of $J_1(\lambda R)$ inside the integral over z' , we recognize a derivative with respect to z' of the exponential factor and integrate by part, we then exchange order of integration, and finally integrate in λ by using Equation (2.12.38.1) in P86. For B_z , the approach is to move the λ in front of $J_0(\lambda R)$ inside the Hankel transform \hat{j}_1 , use the identity $\lambda J_1(\lambda\xi) = -dJ_0(\lambda\xi)/d\xi$, and integrate by parts over ξ . Finally, we invert the order of integration and use again Equation (2.12.38.1) in P86. With this first approach we proved the equivalence of Equation (15) with the *second* expressions for B_R and B_z in Equation (12).

However, there is a second approach that proves the equivalence of Equation (15) with the *first* identities in Equation (12), and that also helps to clarify an important convergence issue. In both the triple integrals in Equation (15) we exchange the order of integration, and we evaluate first the integrals over λ , which belong to the family $\int_0^{\infty} x e^{-px} J_{\mu}(ax) J_{\nu}(bx) dx$, with the aid of Equation (2.12.38.2) in P86, where in particular $p = |\Delta z|$ and $x = \lambda$. It can be proved (for example, by asymptotic expansion of the Bessel functions for large values of their argument) that for $\Delta z = 0$ the two integrals over λ diverge; however, if the limit for $\Delta z \rightarrow 0$ is evaluated after integration, then the first identities in Equation (12) are recovered⁴ after expressing $\partial\mathcal{F}_1/\partial z'$ and $-\partial\mathcal{F}_0/\partial\xi$ in explicit form.

3. Series Solution for the Gravitomagnetic Equations: a Razor-thin Disk with Circular Orbits

Having established the general setting of the problem, we are now in position to discuss the radial dependence of the circular velocity of a test mass (a star or a gas cloud) in the plane of a razor-thin disk made of field stars in circular orbits, so that

$$\begin{aligned} \rho(R, z) &= \Sigma(R)\delta(z), & \mathbf{v} &= v(R)\mathbf{e}_{\varphi}, \\ \mathbf{j} &= \chi(R)\delta(z)\mathbf{e}_{\varphi}, \end{aligned} \quad (16)$$

where $\Sigma(R)$ and $v(R)$ are, respectively, the mass surface density and the circular velocity of the disk, and $\chi(R) = \Sigma(R)v(R)$ is the radial profile of the two-dimensional current; according to the orientation of the coordinate system, a positive v means counterclockwise rotation. From the assumption of circular velocities, it follows necessarily that the modulus of the circular velocity of the test stars and of the rotating disk coincide, i.e., $\|\mathbf{v}_*(R)\| = |v(R)|$, and quite naturally we also assume that $\mathbf{v}_*(R) = v(R)\mathbf{e}_{\varphi}$, i.e., that the test stars rotate as the stars of the disk. From Equation (2), where the field \mathbf{E} is just the Newtonian gravitational field produced by $\Sigma(R)$, and from the fact proved in Section 2.1 that in the $z=0$ plane $\mathbf{B} = B_z(R)\mathbf{e}_z$, we obtain the scalar equation for the circular

⁴ The delicacy of the exchange of the limit with the integral when using Bessel functions is best illustrated in electrodynamics by the case of the magnetic field produced by a circular current loop: if one computes the magnetic field in the plane of the spire after restricting \mathbf{A} to the $z=0$ plane, then \mathbf{B} is predicted to diverge everywhere in the $z=0$ plane. Instead, if the field is computed for $z \neq 0$, and then the limit for $z \rightarrow 0$ is considered, the correct expression is obtained (see also Exercise 5.10 in J98).

velocity v at each radius R :

$$v^2 = v_0^2 + RvB_z[\chi], \quad (17)$$

where v_0 is the circular velocity of the disk in the Newtonian case and where, from Equations (12)–(15), the gravitomagnetic field in the disk plane reduces to the equivalent expressions:

$$B_z[\chi] = \frac{G}{c^2} \times \begin{cases} 16 \int_0^\infty \frac{d\xi \chi(\xi)}{d\xi} \frac{K(k)}{R+\xi} d\xi, & k = \frac{2\sqrt{R\xi}}{R+\xi}, \\ 8\pi \int_0^\infty \lambda J_0(\lambda R) \hat{\chi}_1(\lambda) d\lambda. \end{cases} \quad (18)$$

The general discussion in Sections 2.2–2.3 shows that the first expression contains a logarithmic integrable singularity at $\xi=R$, while in the second the order of integration cannot be exchanged with the Hankel transform $\hat{\chi}_1$ given by Equation (14) applied to $\chi(R)$. Notice that with $B_z[\chi]$ we indicate the linear operator acting on the mass current profile (i.e., on the $v(R)$ profile, if the surface density $\Sigma(R)$ profile is assigned); notice also that Equation (17) is a nonlinear integral equation for $v(R)$, even if obtained in the framework of linearized GR, and it is invariant under the inversion of the rotational field of the disk, $v(R) \rightarrow -v(R)$. In practice, by solving Equation (17) for assigned $\Sigma(R)$, we obtain (at the order of the gravitomagnetic equations) the “self-consistent” circular velocity of the disk produced by the combined effects of the Newtonian field and of the gravitomagnetic potential produced by the rotation curve itself.

For a razor-thin disk of total mass M_d and scale length R_d , it is natural to normalize lengths to R_d , surface densities to M_d/R_d^2 , and velocities to $\sqrt{GM_d/R_d}$; a tilde over a quantity indicates normalization to its associated scale. Accordingly, Equation (17) is recast in dimensionless form as

$$\tilde{v}^2 = \tilde{v}_0^2 + \epsilon \tilde{R} \tilde{v} \mathcal{B}[\tilde{\chi}], \quad \epsilon = \frac{GM_d}{R_d c^2}, \quad (19)$$

where ϵ is a dimensionless parameter arising naturally from the normalization of \mathcal{B} . In fact, from Equation (18) we obtain $B_z = \epsilon \sqrt{GM_d/R_d^3} \mathcal{B}$, where \mathcal{B} is the dimensionless gravitomagnetic field in the disk. Notice that for a disk the parameter ϵ is nothing other than the natural proxy for the quantity v^2/c^2 mentioned in Section 1, where v is a characteristic velocity associated with the Newtonian gravitational field (see the solid lines in Figure 3). Therefore, in real galaxies ϵ is very small: for example, $\epsilon \simeq 10^{-6}$ in a disk galaxy with a characteristic rotational velocity of 300 km s⁻¹. Accordingly, we represent v as a regular asymptotic series in powers of ϵ :

$$v(\epsilon, R) = v_0(R) + \epsilon^\alpha v_1(R) + \mathcal{O}(\epsilon^{2\alpha}), \quad \alpha > 0, \quad (20)$$

where the exponent α is to be fixed by order balance, and of course for $\epsilon \rightarrow 0$ we reobtain the Newtonian case. Inserting the expansion above in Equation (17), from the linearity of $B_z[\chi]$ on velocity, it follows necessarily that $\alpha=1$, and at points

where $\tilde{v}_0 \neq 0$,

$$\tilde{v}_1 = \frac{\tilde{R}}{2} \mathcal{B}[\tilde{\chi}_0], \quad (21)$$

where $\tilde{\chi}_0$ is the (normalized) surface density current profile corresponding to the Newtonian rotation curve \tilde{v}_0 : from $\mathcal{O}(B_z[\tilde{\chi}_0]) = \epsilon$, it follows that the term \tilde{v}_1 depends on the gravitomagnetic field produced by the Newtonian current only. At the origin, the only point⁵ at finite R where \tilde{v}_0 can vanish, perturbation analysis shows that again $\alpha=1$, but $\tilde{v}_1 = \tilde{R} \mathcal{B}[\tilde{\chi}_0]$; however, as $R=0$, no difference arises with Equation (21), which therefore can be used uniformly over the whole radial range. Moreover, Equation (21) shows that the GR corrections due to a counterclockwise current lead to a *decrease* of the rotational speed where $B_z[\chi_0]$ is negative, and an *increase* where $B_z[\chi_0]$ is positive. Of course, it is immediate to verify that the effects on the circular speed are the same for a global inversion of the rotational velocity $v_0 \rightarrow -v_0$, due to the associated change of sign of $B_z[\chi_0]$. It is important to remark that Equation (21) allows for an alternative interpretation: one could just consider the field $B_z[\tilde{\chi}_0]$ at the right-hand side of Equation (17), and then solve in closed form the resulting quadratic equation for $v(R)$. After selecting the sign so that for $\epsilon \rightarrow 0$ the Newtonian profile is reobtained, an expansion of the solution for $\epsilon \rightarrow 0$ and truncation at the first order gives again Equation (21), proving again that the linear gravitomagnetic formulation of the problem leads to a regular perturbation problem (e.g., see Bender & Orszag 1978, Chapter 7).

Of course, even if the problem admits a regular perturbation approach, with a solution reducing to the Newtonian one in the limit $\epsilon=0$, the function \tilde{v}_1 could attain very large (but finite) values, compensating the small (but nonzero) value of ϵ , and producing a perturbation of the same order of magnitude⁶ or even larger than the Newtonian term: this would be a strong support for the possibility of a GR origin of the flat rotation curve of disk galaxies. In the next examples, based on realistic disk density profiles, we show however that this is not the case, and \tilde{v}_1 remains small, with absolute values well below the unity.

3.1. The Exponential Disk

In our first application we consider the razor-thin exponential disk of total mass M_d and scale length R_d , the standard model used to describe the stellar density distribution of disk galaxies (e.g., BT08; Bertin 2014). The surface density is given by

$$\Sigma(R) = \frac{M_d e^{-R}}{R_d^2 2\pi}, \quad \tilde{R} = \frac{R}{R_d}, \quad (22)$$

⁵ A clear distinction should be made between the mass current and the rotation curve: in case of truncated disks the former is spatially limited to the region occupied by the disk, while the latter, and the field $B_z[\chi]$, are defined also in the empty region beyond the disk edge.

⁶ In converging regular expansions higher-order terms can be larger than lower-order terms: as a simple example consider the first two terms of the absolutely converging series $e^{\epsilon x} = 1 + \epsilon x + \mathcal{O}(\epsilon^2 x^2)$, for fixed $\epsilon < \alpha$ and $x > \epsilon$.

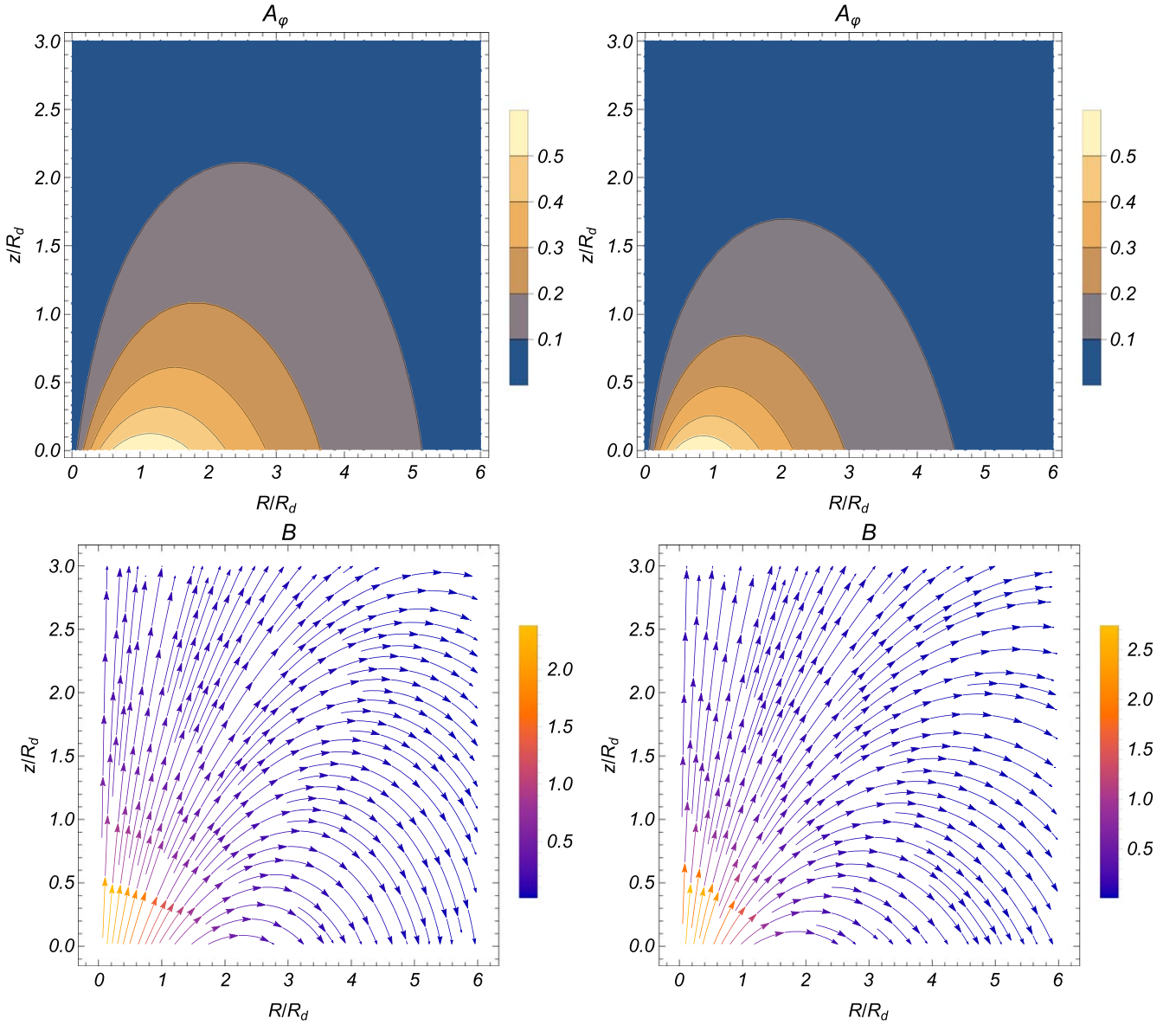


Figure 1. Top panels: the A_φ field for the counterclockwise rotating exponential (left) and Kuzmin (right) razor-thin disks, in units of $\epsilon \sqrt{GM_d/R_d}$, where $\epsilon = GM_d/(R_d c^2)$. The field is computed for the Newtonian current χ_0 , as required by Equation (21), and it looks similar to the field that would be produced by the current of a circular spire; the maximum of the Newtonian current is located at $R_0 \simeq 0.574 R_d$ for the exponential disk, and at $R_0 \simeq 0.535 R_d$ for the Kuzmin disk. The maximum of A_φ is located at $R_A \simeq 1.12 R_d$ for the exponential disk and at $R_A \simeq 0.85 R_d$ for the Kuzmin disk. Bottom panels: the corresponding \mathbf{B} field, in units of $\epsilon \sqrt{GM_d/R_d^3}$. At $z = 0$, B_z is positive in the inner regions of the disk and negative outside; the radius R_B at which $B_z = 0$ is determined by the critical point of $RA_\varphi(R)$, and so does not coincide with the position of the maximum of $A_\varphi(R)$, as apparent from the figures. Numerically, $R_B \simeq 2.2 R_d$ for the exponential disk, and $R_B \simeq 1.68$ for the Kuzmin disk.

and in Newtonian gravity the gravitational potential in the equatorial plane is

$$\phi(R) = -\frac{GM_d}{R_d} \frac{\tilde{R}}{2} \left[I_0\left(\frac{\tilde{R}}{2}\right) K_1\left(\frac{\tilde{R}}{2}\right) - I_1\left(\frac{\tilde{R}}{2}\right) K_0\left(\frac{\tilde{R}}{2}\right) \right], \quad (23)$$

so that the associated circular velocity is

$$v_0^2(R) = \frac{GM_d}{R_d} \frac{\tilde{R}^2}{2} \left[I_0\left(\frac{\tilde{R}}{2}\right) K_0\left(\frac{\tilde{R}}{2}\right) - I_1\left(\frac{\tilde{R}}{2}\right) K_1\left(\frac{\tilde{R}}{2}\right) \right], \quad (24)$$

where I_m and K_m are the modified Bessel functions of order m (e.g., BT08; C21). As already remarked in Section 1, the maximum of v_0 is reached at $R \simeq 2.15 R_d$, and in the range $1.5 < \tilde{R} < 3$ the curve is almost flat even in absence of DM:

notice that inside $3 R_d$ the disk already contains $\simeq 0.8 M_d$. The Newtonian current surface density χ_0 for a disk made by purely circular orbits is then obtained from Equations (22)–(24): for a global counterclockwise rotation, it reaches the maximum at $R_0 \simeq 0.574 R_d$.

For the exponential disk it turns out that the most efficient way to compute the gravitomagnetic field is to use the formulation in terms of elliptic integrals. In particular, as the current density is a regular function of R , the general discussion about convergence leads to use Equation (11) for the evaluation of A_φ , and the first and second integrals in Equation (12) for the evaluation of B_R and B_z , respectively: of course, in the disk plane the latter expression reduces to the first case in Equation (18). Numerically, the integrable divergence at

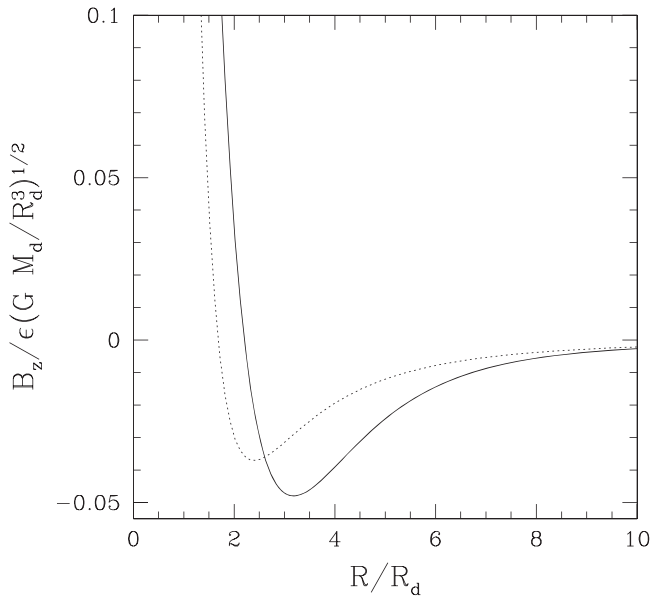


Figure 2. The (dimensionless) gravitomagnetic field \mathcal{B} in the disk plane, for the counterclockwise rotating exponential (solid line), and Kuzmin (dotted line) disks made by purely circular orbits, computed from the Newtonian surface current density χ_0 . B_z in the central regions of the disks is positive, i.e., directed along \mathbf{e}_z , while in the outer parts B_z and \mathbf{e}_z are antiparallel, as also apparent from the bottom panels in Figure 1.

$\xi = R$ is easily treated by splitting the integral from the origin to $(1 - \eta)R$, and from $(1 + \eta)R$ to infinity, and reducing η until acceptable convergence is reached (actually, thanks to absolute convergence, the two η 's do not need to be the same). In the following experiment, convergence was already reached for $\eta = 10^{-3}$, with stable results at 5 significant digits according to Mathematica's NIntegrate function. Importantly, the numerical agreement with the alternative formulation in terms of Bessel functions has been also verified over all the disk.

In the top-left panel of Figure 1, the only nonvanishing component, A_φ , of the potential vector (in units of $\epsilon \sqrt{GM_d/R_d}$), is shown in the meridional plane, where the overall striking similarity with the field produced by an “effective” circular current loop of radius $R_A \simeq 1.12 R_d$ is apparent, where R_A is the position of the maximum of $A_\varphi(R)$; quite obviously, R_A does not coincide with the position R_0 of the maximum of the current. In the bottom-left panel, the associated (normalized) \mathcal{B} field is shown. As expected, the field is similar to that of a circular (counterclockwise circulating) current loop, with B_z positively directed in the inner regions of the disk (where the Biot–Savart fields of each current ring composing χ_0 reinforces), and negatively directed in the outer regions, due to the cooperative (negative) contribution of the current in the inner regions of the disk, while the counteracting positive contributions of the current in the outer regions of the disk are less and less important, due to vanishing of the current at large radii. The radial trend of $B_z[\chi_0]$ in the disk plane is represented by the solid line in Figure 2. Notice that the radius at which $B_z(R) = 0$ is $R_B \simeq 2.2 R_d$, not coincident with R_A , as from Equation (10) R_B is given by the critical point of $R A_\varphi(R)$, while R_A is the critical point of $A_\varphi(R)$. Having determined the field B_z for the exponential disk, from Equation (21) we finally compute v_1 . In the left panel of Figure 3 the solid line shows the (normalized) profile of the Newtonian rotation curve v_0 , while the dotted line gives the perturbative term v_1 . After multiplication by $\epsilon \simeq 10^{-6}$, it is clear that the effects of GR on

the curve of the exponential disk are well below the possibility of any practical detection, with differences with respect to the Newtonian rotation curve well below 1 m s^{-1} : at the descriptive level of gravitomagnetism, GR does not produce any effect on the rotation curve of the disk. In any case, it is interesting to notice that, for the reasons explained above, the sign of the gravitomagnetic field in the Lorentz equation actually produces a *decrease* of the rotational speed at large galactocentric distances!

3.2. The Kuzmin–Toomre Disk

Having determined the solution for the exponential disk, in order to confirm the obtained results we move to explore a different disk model. We focus on the Kuzmin–Toomre razor-thin disk (Kuzmin 1956; Toomre 1963; see also BT08; C21), an idealized model widely used in stellar dynamics for its mathematical simplicity. The surface density–potential pair of a disk of total mass M_d and scale length R_d is given by

$$\begin{aligned} \Sigma(R) &= \frac{M_d}{R_d^2} \frac{1}{2\pi(\tilde{R}^2 + 1)^{3/2}}, \\ \phi(R) &= -\frac{GM_d}{R_d} \frac{1}{\sqrt{\tilde{R}^2 + 1}}, \quad \tilde{R} = \frac{R}{R_d}, \end{aligned} \quad (25)$$

where the potential is restricted to the disk plane, and the Newtonian circular velocity and the surface mass density current are given by

$$\begin{aligned} v_0^2(R) &= \frac{GM_d}{R_d} \frac{\tilde{R}^2}{(\tilde{R}^2 + 1)^{3/2}}, \\ \chi_0(R) &= \sqrt{\frac{GM_d^3}{R_d^5}} \frac{\tilde{R}}{2\pi(\tilde{R}^2 + 1)^{9/4}}. \end{aligned} \quad (26)$$

The maximum of v_0 is located at $R = \sqrt{2}R_d$, and that of χ_0 at $R_0 = \sqrt{2/7}R_d \simeq 0.535 R_d$, a value curiously similar to that of the exponential disk. We now show that v_1 can be obtained in closed form by using the Fourier–Bessel identity in Equation (18). In fact, from Equation (6.565.4) of GR07, or Equation (2.12.4.28) of P86, we obtain the Hankel transform of order 1 for the Newtonian mass current as

$$\hat{\chi}_1(\tilde{\lambda}) = \sqrt{\frac{GM_d^3}{R_d}} \frac{\tilde{\lambda}^{5/4} K_{1/4}(\tilde{\lambda})}{2^{9/4} \pi \Gamma(9/4)}, \quad \tilde{\lambda} = \lambda R_d, \quad (27)$$

where Γ is the complete gamma function, and we used the fact that for modified Bessel functions $K_{-\nu} = K_\nu$; notice that $\tilde{\lambda}$ is a dimensionless quantity. The last integral in Equation (18) can be expressed analytically thanks to Equation (6.576.3) of GR07 or Equation (2.16.21.1) of P86, and finally from Equation (21) we obtain

$$v_1(R) = \sqrt{\frac{GM_d}{R_d}} \frac{2\Gamma(7/4)\Gamma(3/2)}{\Gamma(9/4)} {}_2F_1\left(\frac{7}{4}, \frac{3}{2}; 1; -\tilde{R}^2\right) \tilde{R}, \quad (28)$$

where ${}_2F_1$ is the standard hypergeometric function. Notice that the equation above can be recast in terms of elliptic integrals, resulting in perfect agreement over the whole radial range with the values of $v_1(R)$ obtained from Equation (21) and numerical integration of the last expression of B_z in Equation (12), in a reassuring validity check. As a mathematical curiosity, we also

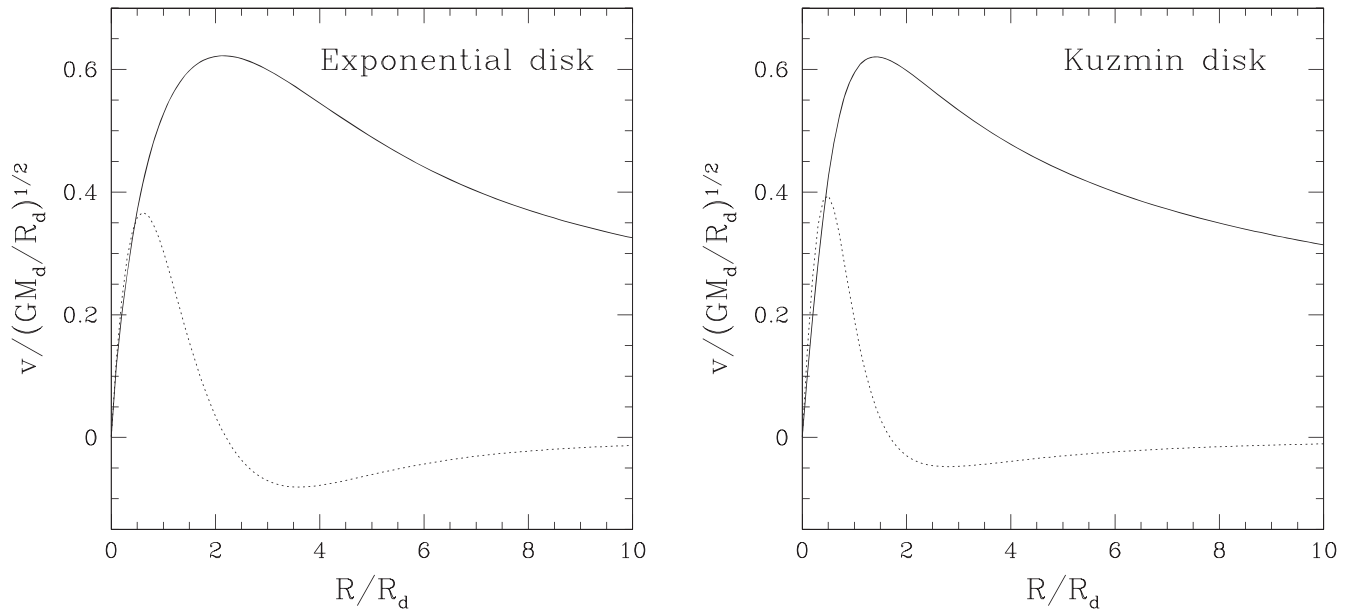


Figure 3. Radial trend of the rotational velocity components in Equation (20) normalized to $\sqrt{GM_d/R_d}$, for the exponential (left) and Kuzmin–Toomre (right) disks. The solid line is the Newtonian rotation curve v_0 , and the dotted line is the v_1 perturbative term, that should then be added to v_0 after multiplication by $\epsilon \simeq 10^{-6}$. Notice how, in principle, the effect of the GR gravitomagnetic field at large radii is a *decrease* of the circular velocity with respect to the Newtonian case.

notice that for the Newtonian current χ_0 of the Kuzmin–Toomre disk, not only the field B_z in the disk plane can be obtained explicitly but also Equations (15) can be solved analytically over the whole space by using Fox H functions after expressing Equation (27) in terms of these functions (e.g., Mathai et al. 2010, and in particular Equation (2.25.3.2) in Prudnikov et al. 1990): the resulting expression is, however, of no practical use, and so not reported here.

In the right panels of Figure 1 we plot the normalized potential vector of the disk in the meridional plane and the associated gravitomagnetic field: the maximum of the gravitomagnetic potential vector is reached at $R_A \simeq 0.85 R_d$. The similarity with the case of the exponential disk, and also the range of values spanned by the normalized fields, is remarkably similar, even if the radial density profiles of the two disks are quite different, especially at large radii; notice also the similar behavior of B_z in Figure 2, with positive values in the inner regions of the disk (i.e., for $R < R_B \simeq 1.68$), and negative values outside. In Figure 3 we plot the normalized profiles of v_0 and v_1 . It is again apparent how v_1 remains limited over all the radial range, confirming that the contribution to the rotational velocity of the first-order perturbative term in the velocity expansion is fully controlled by the smallness of ϵ , and again the expected GR corrections to the Newtonian rotational velocity of the galaxy are well below the detection limit, with differences between the Newtonian and the gravitomagnetic GR curve well below 1 m s^{-1} . Finally, in accordance with the change of sign of B_z along the equatorial plane, the gravitomagnetic effects produce a decrease⁷ of the rotational speed at large distances from the galaxy center.

Therefore, from the analysis conducted so far, it seems a quite robust conclusion that GR, at the level of the gravitomagnetic weak-field approximation, does not affect the

rotation curve of self-gravitating baryonic disks with realistic density profiles, and made mostly by circular orbits. In the next section we relax the assumption of a two-dimensional density distribution, and we also consider noncircular orbits for the stars producing the field in the system.

4. The Gravitomagnetic Jeans Equations

After the discussion of razor-thin disks, we address the problem of the expected effects of GR on the internal dynamics of genuinely tridimensional (collisionless) astronomical systems, such as finite-thickness disk galaxies or axisymmetric elliptical galaxies. We first rigorously derive the gravitomagnetic modification of the Jeans equations, and then we restrict to stationary axisymmetric systems. As usual, we indicate with \mathbf{v} the phase-space velocity, so that the density ρ and the streaming velocity field \mathbf{v} of the system are given by

$$\begin{aligned} \rho(\mathbf{x}) &= \int f d^3 \mathbf{v}, \\ \mathbf{v}(\mathbf{x}) \equiv \bar{\mathbf{v}} &= \frac{1}{\rho(\mathbf{x})} \int f \mathbf{v} d^3 \mathbf{v}, \end{aligned} \quad (29)$$

where $f(\mathbf{x}, \mathbf{v}, t)$ is the phase-space distribution function (hereafter DF; see BT08; Bertin 2014; C21), and a bar over a quantity indicates its average over the velocity space. In the following we will write $\mathbf{v} = v_i \mathbf{e}_i = v_R \mathbf{e}_R + v_\varphi \mathbf{e}_\varphi + v_z \mathbf{e}_z$, and $\mathbf{v} = v_i \mathbf{e}_i = v_R \mathbf{e}_R + v_\varphi \mathbf{e}_\varphi + v_z \mathbf{e}_z$, where sums over repeated indices hold in Cartesian coordinates.

Suppose the considered stellar system is self-consistent, i.e., the motion of each star is determined by the field produced by the combined effects of all the other stars. As we are in the low-velocity limit, when the Biot–Savart law can be interpreted as the sum of the Lorentz fields produced by each moving charge (an interpretation in general *not* true for currents produced by particles of arbitrary large velocities; see, e.g., J98, Chapter 5; Griffiths 1999, Chapter 5; Feynman et al. 1977, Chapters 13 and 21; Panofsky & Phillips 1962, Chapter 7), it follows that

⁷ The change of sign of $B_z(R)$ is not a universal property: for example, it is quite easy to prove that in razor-thin power-law disks (and so of infinite total mass), with a uniform sense of rotation, the gravitomagnetic field in the disk cannot change sign with R .

the acceleration experienced by a star at \mathbf{x} with velocity \mathbf{v} can be written by summing the right-hand side member of Equation (2) over the DF,

$$\begin{aligned} \frac{d^2\mathbf{x}}{dt^2} &= -\nabla\phi - \mathbf{v} \wedge \mathbf{B}[\mathbf{j}], \\ \mathbf{j}(\mathbf{x}) &= \rho\mathbf{v} = \int f\mathbf{v}d^3\mathbf{v}, \end{aligned} \quad (30)$$

where $\phi(\mathbf{x})$ is the Newtonian gravitational potential of the system and $\mathbf{B}[\mathbf{j}]$, by virtue of the linearity of \mathbf{B} on the current, is the gravitomagnetic field produced at \mathbf{x} by the total streaming current of the system. The hierarchy of the Jeans equations of increasing order is then obtained by taking moments over the velocity space of the collisionless Boltzmann equation (e.g., see BT08; C21):

$$\frac{\partial f}{\partial t} + v_i \frac{\partial f}{\partial x_i} + \frac{dv_i}{dt} \frac{\partial f}{\partial v_i} = 0, \quad (31)$$

here written in Cartesian coordinates. After multiplication of Equation (31) by 1, v_i , $v_i v_j$, etc., and integration, the three second-order moments equations (the gravitomagnetic modification of the usual Jeans equations of stellar dynamics) are given by

$$\begin{aligned} \frac{\partial \rho v_i}{\partial t} + \frac{\partial \rho \overline{v_i v_k}}{\partial x_k} &= -\rho \frac{\partial \phi}{\partial x_i} - \epsilon_{ijk} \rho v_j B_k[\mathbf{j}], \\ i &= 1, 2, 3, \end{aligned} \quad (32)$$

where

$$\begin{aligned} \overline{v_i v_j}(\mathbf{x}) &= \frac{1}{\rho(\mathbf{x})} \int f v_i v_j d^3\mathbf{v}, \\ \sigma_{ij}^2(\mathbf{x}) &= \overline{(v_i - v_i)(v_j - v_j)} = \overline{v_i v_j} - v_i v_j. \end{aligned} \quad (33)$$

In particular, σ_{ij}^2 are the components of the second-order velocity dispersion tensor. In Appendix B, the general gravitomagnetic time-dependent Jeans equations are also reported in cylindrical coordinates.

We now proceed to restrict to the axisymmetric stationary case. In the usual stellar dynamical case, from the Jeans theorem one would assume a phase-space DF depending on the two classical integrals of the motion (per unit mass) E and J_z , i.e., the orbital energy and the z -component of the angular momentum of stellar orbits. As is well known, under this assumption (e.g., BT08; C21), important constraints on the allowed velocity moments follow, namely (1) the only possible streaming motions are in the azimuthal direction, i.e., $\mathbf{v} = v_\varphi(R, z)\mathbf{e}_\varphi$, and (2) the velocity dispersion tensor is in diagonal form at each point in the system, with $\sigma_R^2 = \sigma_z^2 \equiv \sigma^2$, while only $\overline{v_\varphi^2} = \sigma_\varphi^2 + v_\varphi^2$ remains determined; when $\sigma_\varphi^2 = \sigma^2$ everywhere, the system is said to be isotropic. Therefore, for stationary, stellar dynamical, two-integral axisymmetric systems with $f(E, J_z)$, the current would be of the ‘‘circular type’’ considered in Equation (7), with $\mathbf{j} = \mathbf{j}\mathbf{e}_\varphi = \rho v_\varphi \mathbf{e}_\varphi$; notice that, even if the current associated with the streaming velocity field is circular, the orbits of the individual stars contributing to the resulting gravitomagnetic field are in general *not* circular, and so we are considering an orbital structure more complicated than that of the razor-thin disk in Section 3.

However, in the case of stationary collisionless stellar systems with gravitomagnetic forces, the situation is not so

simple, because while E is still an integral of motion, J_z is not conserved along orbits and so it cannot be used as an isolating integral in the DF. Fortunately, the problem is solved as follows. As is well known, the Lagrangian (per unit mass) associated with Equation (30) is

$$\mathcal{L} = \frac{\|\mathbf{v}\|^2}{2} - (\phi + \mathbf{A} \cdot \mathbf{v}), \quad (34)$$

where, at variance with the EM case (e.g., see Landau & Lifshitz 1971), the + sign in the generalized potential derives from the – sign in the gravitomagnetic Lorentz force. Suppose now that $\mathbf{v} = v_\varphi(R, z)\mathbf{e}_\varphi$, so that $\mathbf{A} = A_\varphi(R, z)\mathbf{e}_\varphi$ from the results in Section 2.1. The Euler–Lagrange equations show immediately that J_z is not conserved, but a second integral of motion exists, $I_2 = J_z - RA_\varphi$. The Jeans theorem then in principle allows for a two-integral DF, $f(E, I_2)$, and an interesting question arises whether such a DF is consistent with the assumption of streaming motions with $\mathbf{v} = v_\varphi(R, z)\mathbf{e}_\varphi$ used to prove the existence of I_2 . The answer is in the affirmative, and it is easy to prove that properties (1) and (2) mentioned above for systems supported by a $f(E, J_z)$ are preserved by the generalized $f(E, I_2)$, in particular the fact that $v_R = v_z = 0$. Therefore, the vertical and radial Jeans Equations (B2) for a stationary, axisymmetric two-integral system with gravitomagnetic forces, supported by a DF of the family $f(E, I_2)$, become

$$\begin{cases} \frac{\partial \rho \sigma^2}{\partial z} = -\rho \frac{\partial \phi}{\partial z} + j B_R[j], & j = \rho v_\varphi, \\ \frac{\partial \rho \sigma^2}{\partial R} - \frac{\rho \Delta}{R} = -\rho \frac{\partial \phi}{\partial R} - j B_z[j], \end{cases} \quad (35)$$

where $\Delta = \overline{v_\varphi^2} - \sigma^2$, and in the isotropic rotator case $\Delta = v_\varphi^2$. Finally, the azimuthal Jeans equation vanishes identically also in the gravitomagnetic case, as obvious from the last of Equations (B2). Notice how, at variance with the classical Newtonian case, now the vertical and radial velocity dispersions depend on the ordered rotational field $v_\varphi(R, z)$, yet to be determined.

Equations (35) can be formally solved in terms of σ^2 and Δ as in the usual stellar dynamical case, obtaining

$$\begin{aligned} \rho \sigma^2 &= \int_z^\infty \rho \frac{\partial \phi}{\partial z'} dz' - U = \rho \sigma_0^2 - U, \\ U(R, z) &= \int_z^\infty j B_R[j] dz', \end{aligned} \quad (36)$$

where σ_0^2 is the Newtonian solution, and $U(R, z)$ accounts for the gravitomagnetic effects. Moreover, some algebra shows that

$$\begin{aligned} \frac{\rho \Delta}{R} &= C[\rho, \phi] - V, \\ C[\rho, \phi] &= \int_z^\infty \left(\frac{\partial \rho}{\partial R} \frac{\partial \phi}{\partial z'} - \frac{\partial \rho}{\partial z'} \frac{\partial \phi}{\partial R} \right) dz' = \frac{\rho \Delta_0}{R}, \end{aligned} \quad (37)$$

where the commutator $C[\rho, \phi]$ is the standard Newtonian solution (e.g., Hunter 1977; Barnabè et al. 2006; see also C21),

while the term

$$\begin{aligned} V(R, z) &= \int_z^\infty \left(\frac{\partial j B_R}{\partial R} + \frac{\partial j B_z}{\partial z'} \right) dz' \\ &= \int_z^\infty \left[\left(\frac{\partial}{\partial R} \frac{j}{R} \right) R B_R + \frac{\partial j}{\partial z'} B_z \right] dz' \\ &= -C[j, A_\varphi] - \frac{j A_\varphi}{R} \end{aligned} \quad (38)$$

contains the gravitomagnetic effects. The triple integral in the second expression above (obtained from the first by exploiting the solenoidal nature of \mathbf{B}) is particularly well suited for numerical computations when the current is analytically available (see next section), while the last expression is obtained from the first taking into account that $\mathbf{B} = \nabla \wedge \mathbf{A}$, Equation (10), and finally integrating by parts with $j A_\varphi = 0$ for $z \rightarrow \infty$.

As noticed, the difficulty in the solution of the gravitomagnetic Jeans equations is the fact that the force field depends on the azimuthal streaming velocity distribution, a quantity that it is not known in advance. In principle, to solve the gravitomagnetic Jeans equations one should (1) impose a decomposition on the still-unknown azimuthal velocity field, for example by using the widely adopted Satoh (1980) ansatz $v_\varphi^2 = k^2 \Delta$ (e.g., see C21), (2) solve the resulting nonlinear integrodifferential Equation (37) for v_φ and obtain $B_R[j]$, (3) integrate Equation (36) and obtain σ^2 , (4) conclude by determining Δ and the tangential velocity dispersion $\sigma_\varphi^2 = \sigma^2 + (1 - k^2)\Delta = \sigma^2 + (1/k^2 - 1)v_\varphi^2$. Quite obviously, a considerable simplification is achieved by exploiting the fact that in Equation (35) the fields B_R and B_z are proportional to the small parameter $\epsilon = GM_*/(r_* c^2)$, where M_* is the total mass of the system, and r_* its scale length. As in the razor-thin disks, it follows immediately that the first-order perturbative terms in the natural expansions $\sigma^2 = \sigma_0^2 + \epsilon \sigma_1^2 \dots$, $\Delta = \Delta_0 + \epsilon \Delta_1 \dots$, and $v_\varphi = v_{\varphi 0} + \epsilon v_{\varphi 1} \dots$, are related to the functions U and V evaluated over the Newtonian current $j_0 = \rho v_{\varphi 0}$, where $v_{\varphi 0}(R, z)$ is the streaming rotation velocity obtained from the classical Jeans equations.

We are now in a position to evaluate the effects of GR corrections on the circular velocity $v(\epsilon, R) = v_0(R) + \epsilon v_1(R) + \dots$ of a test star in the equatorial plane of an axisymmetric collisionless system described by Equation (35). The only difference with the razor-thin disks in Section 3 is that now the current is provided by the azimuthal streaming velocity field of the system. From Equation (30), the analogies of Equations (17) and (19) still apply, and

$$\tilde{v}_1 = \frac{\tilde{R}}{2} \mathcal{B}[j_0], \quad (39)$$

$B_z = \epsilon \sqrt{GM_*/r_*^3} \mathcal{B}$ is computed in the disk plane, and finally $j_0 = \sqrt{GM_*^3/r_*^7} \tilde{j}_0$.

The expression for the first-order correction term to the streaming velocity (restricting for simplicity to an isotropic rotator case for the stellar distribution of the galaxy) is instead obtained from Equation (37), considering that at the lowest order $V = \mathcal{O}(\epsilon)$, and so from $v_\varphi = v_{\varphi 0} + \epsilon v_{\varphi 1} \dots$, after order balance and some simplification, one gets

$$\tilde{v}_{\varphi 1} = -\frac{\tilde{R}}{2j_0} \mathcal{V}[j_0], \quad (40)$$

where $V = \epsilon (GM_*^2/r_*^5) \mathcal{V}$ is computed from Equation (38).

4.1. The Miyamoto–Nagai Disk

We now solve the gravitomagnetic Jeans equations, and evaluate Equations (39)–(39) for the widely used Miyamoto–Nagai (Miyamoto & Nagai 1975; Nagai & Miyamoto 1976; see also BT08; C21) disk of total mass M_* and scale lengths a and b , with the Newtonian density–potential pair:

$$\begin{aligned} \rho(R, z) &= \frac{M_*}{a^3} \frac{s^2}{4\pi} \frac{\tilde{R}^2 + (1 + 3\zeta)(1 + \zeta)^2}{\zeta^3 [\tilde{R}^2 + (1 + \zeta)^2]^{5/2}}, \\ \phi(R, z) &= -\frac{GM_*}{a} \frac{1}{\sqrt{\tilde{R}^2 + (1 + \zeta)^2}}, \end{aligned} \quad (41)$$

where $\zeta = \sqrt{\tilde{z}^2 + s^2}$, $\tilde{R} = R/a$, $\tilde{z} = z/a$, and the Newtonian circular velocity in the equatorial plane is given by

$$v_0^2(R) = \frac{GM_*}{a} \frac{\tilde{R}^2}{[\tilde{R}^2 + (1 + s)^2]^{3/2}}. \quad (42)$$

The dimensionless parameter $s = b/a$ measures the disk flattening, and for $b = 0$ the model reduces to a Kuzmin disk of total mass M_* and scale length a , so we are in a condition to explore the GR effects of a nonzero thickness on the rotation curve, by comparison with the case in Section 3.2.

We restrict for simplicity to an isotropic rotator, with a counterclockwise streaming velocity field, so that the Newtonian azimuthal streaming velocity field and the associated current density are

$$\begin{cases} v_{\varphi 0}^2(R, z) = \frac{GM_*}{a} \frac{\tilde{R}^2}{[\tilde{R}^2 + (1 + 3\zeta)(1 + \zeta)^2] \sqrt{\tilde{R}^2 + (1 + \zeta)^2}}, \\ j_0(R, z) = \sqrt{\frac{GM_*^3}{a^7}} \frac{s^2}{4\pi} \frac{\tilde{R} \sqrt{\tilde{R}^2 + (1 + 3\zeta)(1 + \zeta)^2}}{\zeta^3 [\tilde{R}^2 + (1 + \zeta)^2]^{1/4}} \end{cases} \quad (43)$$

(e.g., Ciotti & Pellegrini 1996; Smet et al. 2015). Notice that in the equatorial plane the location of the maximum of $j_0(R, 0)$ can be evaluated analytically as a biquadratic equation, and for $s \rightarrow 0$ the position coincides with that of the maximum for the Kuzmin disk.

In the left panel of Figure 4 we show the results for the circular velocity, to be compared with the analogous Figure 3 for the two razor-thin disks made by circular orbits. The solid line represents the Newtonian circular velocity \tilde{v}_0 in Equation (42), while the dotted line gives the correction term in Equation (39), where the gravitomagnetic field is now produced by stars that in general are not moving in circular orbits. Again, for realistic mass distributions, the perturbation term should be multiplied by factor $\epsilon \approx 10^{-6}$ before addition to the Newtonian term: the GR effects appear again to be completely negligible and, in analogy with the case of razor-thin disks, positive in the inner regions of the galaxy and negative at large radii, *reducing* there the rotational speed of a test mass. In the right panel we show, instead, the streaming velocity of stars in the disk equatorial plane, both the Newtonian component (solid line), and the lowest-order GR term (dotted line). Again, it is important to remark that the orbits of the individual stars producing the v_φ

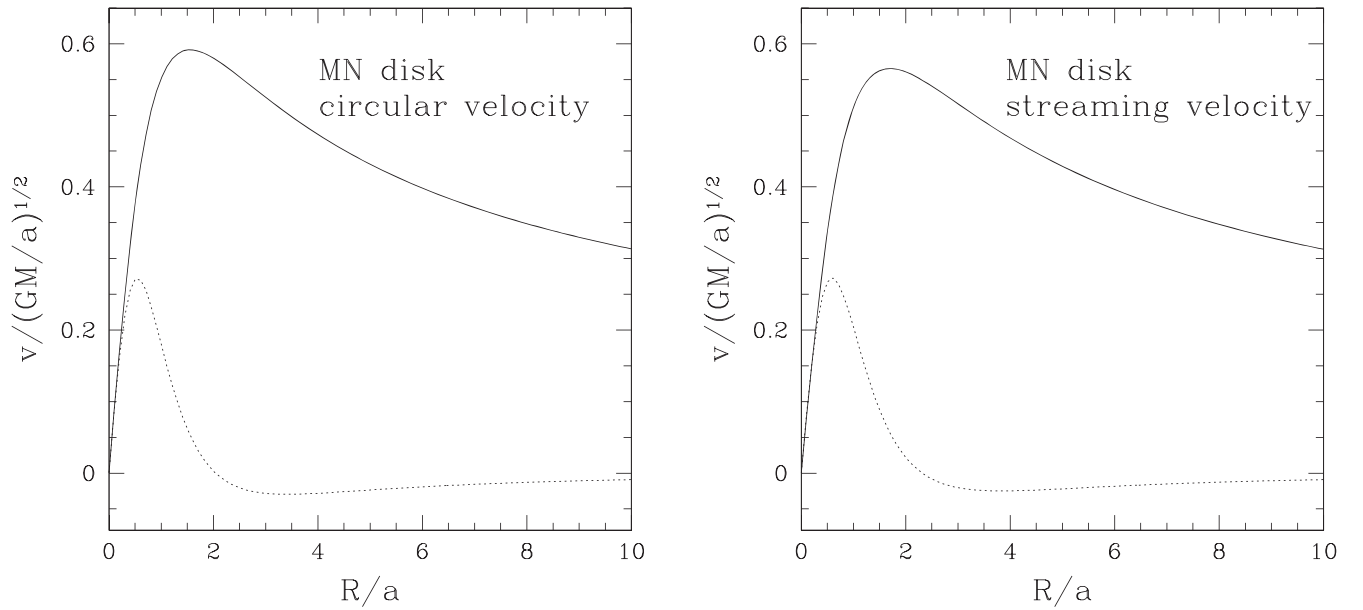


Figure 4. Radial trend of the rotational velocity components (left), and of the streaming velocity (right), normalized to $\sqrt{GM_*/a}$, in the equatorial plane of the counterclockwise rotating isotropic Miyamoto–Nagai disk with flattening parameter $s = b/a = 0.1$. The solid lines are the Newtonian components, and the dotted lines are the first perturbative term, which should be added to the corresponding Newtonian term after multiplication by $\epsilon \simeq 10^{-6}$. Note how the circular velocity is slightly larger than the streaming velocity, the well-known phenomenon of asymmetric drift produced by the disk vertical velocity dispersion support.

in the equatorial plane are in general *not* circular, and not restricted to the equatorial plane. Notice how the Newtonian streaming velocity is slightly below the Newtonian circular velocity, the well-known phenomenon of *asymmetric drift*, due to effect of the vertical component of the velocity dispersion tensor (e.g., see BT08). Notice also how the asymmetric drift (a small but well-measured phenomenon in real galaxies) is several orders of magnitude larger than the GR corrections.

The results for the Miyamoto–Nagai disk reinforce the previous conclusions, i.e., also in three-dimensional galaxies, with stars moving on noncircular orbits, the GR effects predicted by linear gravitomagnetism on the rotational velocities are a factor of $\approx 10^{-6}$ smaller than the Newtonian predictions. If Newtonian gravity requires DM, unless “strong” weak-field GR effects (beyond the linear gravitomagnetic description) actually dominates the dynamics of the galaxies, exactly the same amount and distribution of DM is required in GR and in Newtonian gravity, in order to reproduce the observed rotational curves.

5. Discussion and Conclusions

Recently, it has been suggested that the observed flat radial profile of the rotation curves of disk galaxies at large galactocentric radii could be a peculiar effect of GR in rotating systems, instead of the dynamical signature of the presence of DM halos. The suggestion is somewhat puzzling, as observed galaxies are empirically in a weak-field regime, with $v/c \approx 10^{-3}$, and so GR corrections are expected to be very small; however, GR is a nonlinear theory, and so important effects cannot be excluded in principle.

In this paper, instead of attempting a GR modelization of the rotation curve of some observed galaxy, we followed a different approach, and we built rotation curves for purely baryonic disks, structurally resembling real galaxies, and with total mass and scale length in the observed range. The rotation

curves are computed both in Newtonian gravity and in the (gravitomagnetic) weak-field formulation of GR, and then compared. After a detailed discussion of the mathematics, we considered first the case of razor-thin disks made by purely circular orbits. The orbital structure is highly idealized, but the surface density of the disk is the standard exponential profile adopted to model the stellar distribution in real disk galaxies; we also considered another disk model, the Kuzmin–Toomre model, to gain confidence with the results obtained for the exponential disk. Consistent with the gravitomagnetic approximation adopted, we impose “self-consistency” on the rotational velocity, i.e., we assume that the rotational velocity of the test particle (star or gas cloud) and the rotational velocity of the stellar population producing the gravitomagnetic field are the same at each radius, and we require that the rotational velocity is the solution of the Lorentz-like equation of motion. The resulting problem is shown to be a regular perturbation problem, with an intrinsic order parameter $\epsilon \approx 10^{-6}$, and the gravitomagnetic field is obtained from two different (but equivalent) methods, i.e., by using elliptic integrals and Bessel functions. It is found that the GR (normalized) perturbative term is of the order of unity, with no indications of anomalously large emerging effects, and the resulting physical modification of the Newtonian rotation curve is therefore of the order $\epsilon \approx 10^{-6}$, well below the possibility of detection in observed rotation curves, in agreement with the order-of-magnitude estimate obtained by Toth (2021). Curiously, in the external regions of the disk the gravitomagnetic GR perturbative term tends to *decrease* the rotational speed, as can easily be understood by considering the gravitomagnetic field as given by the sum of the fields produced by each current ring of the disk, and by the fact that the disk current in *realistic* disk galaxies decreases sufficiently fast at increasing radius, so that in the outer regions of the disk the gravitomagnetic field is dominated by the inner current distribution. An important warning follows: if one assumes a disk surface density

distribution with a sufficiently slow radial decline at increasing R , it is quite easy to show that the sum of the fields of *external* rings can be very large (or even diverge), leading to the wrong conclusion of a significant GR effect in real galaxies; in theoretical/numerical studies of the present problem, the use of *realistic* density profiles for the disks is of fundamental importance.

As doubts have been casted that disk thickness effects, or motions more complicated than purely circular orbits for the stars producing the gravitomagnetic fields, could be important, we also studied the case of gravitomagnetic rotation curves in genuinely tridimensional stellar systems. We first derived the gravitomagnetic Jeans equations starting directly from the collisionless Boltzmann equation, and the associated Jeans theorem. In this case the equations naturally contain a vertical “pressure” term due to the vertical velocity dispersion. We showed how in axisymmetric systems the gravitomagnetic field depends on the azimuthal streaming velocity field of the system (even though the orbits of the single stars are in general *not* axisymmetric). In such a system, we can identify two different rotational velocities: the circular velocity of a tracer in the equatorial plane, and the (circular) streaming velocity of the stellar population producing the gravitomagnetic field. For both cases we found that the GR perturbative term, after multiplication by the expansion parameter $\epsilon \approx 10^{-6}$, is completely negligible over the Newtonian term, so that also for collisionless axisymmetric systems the GR effects due to rotation appear to be well below detectability, and unable to reproduce a flat rotation curve at large radii any better than a Newtonian model in absence of DM.

In conclusion, the study conducted in this paper excludes the possibility that gravitomagnetic GR effects can compensate by any detectable amount the Keplerian fall of the rotational velocity that would characterize disk galaxies at large distances in absence of DM halos, and produce the observed flat profiles: from the observational point of view, in rotating disk galaxies DM is required by GR exactly as in Newtonian gravity. Of course, if a full GR simulation for the same baryonic disks used in this papers (with disk parameters corresponding to the observed weak-field regime of real galaxies) convincingly proves the opposite, then among other things we should conclude that gravitomagnetic weak-field approximation of GR *cannot* be used to describe the weak-field regime in rotating galactic disks.

I thank Giuseppe Bertin, Antonio Mancino, Bahram Mashhoon, Jerry Ostriker, Silvia Pellegrini, Francesco Pegoraro, Renzo Sancisi, Massimo Stiavelli, and an anonymous referee for important comments. Alberto Parmeggiani (Department of Mathematics of Bologna University), is especially thanked for discussions about some mathematical aspects of this work.

Appendix A Mathematical Identities

Here we list the most important mathematical identities used in this work (see, e.g., BT08; C21; J98, and references therein). The rotor of a vector function in cylindrical coordinates is

given by

$$\begin{aligned} \nabla \wedge \mathbf{A} = & \left(\frac{1}{R} \frac{\partial A_z}{\partial \varphi} - \frac{\partial A_\varphi}{\partial z} \right) \mathbf{e}_R + \\ & \left(\frac{\partial A_R}{\partial z} - \frac{\partial A_z}{\partial R} \right) \mathbf{e}_\varphi + \frac{1}{R} \left(\frac{\partial R A_\varphi}{\partial R} - \frac{\partial A_R}{\partial \varphi} \right) \mathbf{e}_z. \end{aligned} \quad (\text{A1})$$

The complete elliptic integrals of first and second kind in Legendre form are given, respectively, by

$$\begin{cases} \mathbf{K}(k) = \int_0^{\pi/2} \frac{d\varphi'}{\sqrt{1 - k^2 \sin^2 \varphi'}} = \int_0^1 \frac{dt}{\sqrt{(1-t^2)(1-k^2 t^2)}}, \\ \mathbf{E}(k) = \int_0^{\pi/2} \sqrt{1 - k^2 \sin^2 \varphi'} d\varphi' = \int_0^1 \sqrt{\frac{1 - k^2 t^2}{1 - t^2}} dt; \end{cases} \quad (\text{A2})$$

and, from Equation (8.123) of GR07,

$$\begin{cases} \frac{d\mathbf{K}(k)}{dk} = \frac{\mathbf{E}(k)}{k(1-k^2)} - \frac{\mathbf{K}(k)}{k}, \\ \frac{d\mathbf{E}(k)}{dk} = \frac{\mathbf{E}(k) - \mathbf{K}(k)}{k}. \end{cases} \quad (\text{A3})$$

The two integrals over φ' in Equations (8)–(9) leading to Equations (11)–(12), after reduction to the first quadrant with the bisection formula $\cos \varphi' = 2 \cos^2(\varphi'/2) - 1$, become

$$\begin{aligned} \mathcal{F}_0 &= \int_0^{2\pi} \frac{d\varphi'}{\sqrt{R^2 + \xi^2 - 2R\xi \cos \varphi' + \Delta z^2}} \\ &= \frac{4\mathbf{K}(k)}{\sqrt{(R + \xi)^2 + \Delta z^2}}, \end{aligned} \quad (\text{A4})$$

$$\begin{aligned} \mathcal{F}_1 &= \int_0^{2\pi} \frac{\cos \varphi' d\varphi'}{\sqrt{R^2 + \xi^2 - 2R\xi \cos \varphi' + \Delta z^2}} \\ &= \frac{4}{\sqrt{(R + \xi)^2 + \Delta z^2}} \left[\left(\frac{2}{k^2} - 1 \right) \mathbf{K}(k) - \frac{2\mathbf{E}(k)}{k^2} \right], \end{aligned} \quad (\text{A5})$$

where⁸

$$k^2 = \frac{4R\xi}{(R + \xi)^2 + \Delta z^2}, \quad \Delta z = z - z'. \quad (\text{A6})$$

For the considerations in Sections 2.1 and 2.2, we recall the important identity

$$-\frac{\partial \mathcal{F}_0}{\partial \xi} = \frac{1}{R} \frac{\partial R \mathcal{F}_1}{\partial R}, \quad (\text{A7})$$

which can be proved by differentiation of the explicit expressions in Equations (A4)–(A5), or (with some work) more elegantly directly from their integral representation.

In numerical applications, when using Equations (11)–(12), it is important to recall that $\mathbf{E}(k) \sim 1$ for $k \rightarrow 1^-$, but $\mathbf{K}(k) \sim -\ln \sqrt{1 - k^2} \sim -\ln \sqrt{1 - k}$, so that near the ring

⁸ Notice that, in Mathematica, $\mathbf{K}(k) = \text{EllipticK}[k^2]$, and $\mathbf{E}(k) = \text{EllipticE}[k^2]$.

$\xi = R$ in the $\Delta z = 0$ plane both \mathcal{F}_0 and \mathcal{F}_1 diverge as

$$\mathcal{F}_0 \sim \mathcal{F}_1 \sim \begin{cases} -\frac{4 \ln|R - \xi|}{R + \xi}, & \Delta z = 0, \quad \xi \rightarrow R; \\ -\frac{2 \ln|\Delta z|}{R}, & \xi = R, \quad \Delta z \rightarrow 0; \end{cases} \quad (\text{A8})$$

however, the singularity is integrable and easily treated numerically.

From the theory of Green functions it is possible to prove that in cylindrical coordinates (e.g., BT08; C21)

$$\frac{1}{\|\mathbf{x} - \mathbf{y}\|} = \sum_{m=-\infty}^{\infty} e^{im(\varphi - \varphi')} \int_0^{\infty} \times e^{-\lambda|\Delta z|} J_m(\lambda R) J_m(\lambda \xi) d\lambda, \quad (\text{A9})$$

where J_m are the Bessel functions of first kind and integer order m , $\mathbf{x} = (R \cos \varphi, R \sin \varphi, z)$, $\mathbf{y} = (\xi \cos \varphi', \xi \sin \varphi', z')$, and the Hankel transform for a function $f(R)$ of the cylindrical radius reads

$$\begin{aligned} \hat{f}_m(k) &= \int_0^{\infty} R J_m(\lambda R) f(R) dR, \\ f(R) &= \int_0^{\infty} \lambda J_m(\lambda) \hat{f}_m(\lambda) d\lambda. \end{aligned} \quad (\text{A10})$$

Appendix B

Gravitomagnetic Jeans Equations in Cylindrical Coordinates

By using the standard approach of considering velocity moments of Equation (31), and by working on cylindrical coordinates, from the velocity moment of order 0 we obtain the continuity equation

$$\frac{\partial \rho}{\partial t} + \frac{1}{R} \frac{\partial R \rho v_R}{\partial R} + \frac{1}{R} \frac{\partial \rho v_\varphi}{\partial \varphi} + \frac{\partial \rho v_z}{\partial z} = 0, \quad (\text{B1})$$

and, from the three moments of order 1 (respectively, over v_z , v_R , and v_φ), the three momentum equations:

$$\begin{cases} \frac{\partial \rho v_z}{\partial t} + \frac{1}{R} \frac{\partial R \rho \overline{v_R v_z}}{\partial R} + \frac{1}{R} \frac{\partial \rho \overline{v_\varphi v_z}}{\partial \varphi} + \frac{\partial \rho \overline{v_z^2}}{\partial z} = -\rho \frac{\partial \phi}{\partial z} - \rho (v_R B_\varphi - v_\varphi B_R), \\ \frac{\partial \rho v_R}{\partial t} + \frac{\partial \rho \overline{v_R^2}}{\partial R} - \frac{\rho (\overline{v_\varphi^2} - \overline{v_R^2})}{R} + \frac{1}{R} \frac{\partial \rho \overline{v_R v_\varphi}}{\partial \varphi} + \frac{\partial \rho \overline{v_R v_z}}{\partial z} = -\rho \frac{\partial \phi}{\partial R} - \rho (v_\varphi B_z - v_z B_\varphi), \\ \frac{\partial \rho v_\varphi}{\partial t} + \frac{1}{R^2} \frac{\partial R^2 \rho \overline{v_R v_\varphi}}{\partial R} + \frac{1}{R} \frac{\partial \rho \overline{v_\varphi^2}}{\partial \varphi} + \frac{\partial \rho \overline{v_\varphi v_z}}{\partial z} = -\rho \frac{\partial \phi}{\partial \varphi} - \rho (v_z B_R - v_R B_z), \end{cases} \quad (\text{B2})$$

where the \mathbf{B} field is determined by Equation (3) computed over the galaxy streaming mass density current given by the second of Equation (30). Finally, if the system is in steady state, and supported by a phase-space DF $f(E, J_z - R A_\varphi)$, from the discussion in Section 4 it follows that Equation (B1) and the last of Equations (B2) are identically verified, while the first two of Equations (B2) reduce to Equation (35).

ORCID iDs

Luca Ciotti  <https://orcid.org/0000-0002-5708-5274>

References

- Astesiano, D., & Ruggiero, M. L. 2022, *PhRvD*, **106**, 044061
Balasin, H., & Grumiller, D. 2008, *IIMPD*, **17**, 475
Barnabè, M., Ciotti, L., Fraternali, F., & Sancisi, R. 2006, *A&A*, **446**, 61
Bender, C. M., & Orszag, S. 1978, *Advanced Mathematical Methods for Scientists and Engineers* (New York: McGraw-Hill)
Bertin, G. 2014, *Dynamics of Galaxies* (2nd ed.; Cambridge: Cambridge Univ. Press)
Binney, J., & Tremaine, S. 2008, *Galactic Dynamics* (2nd ed.; Princeton, NJ: Princeton Univ. Press) (BT08)
Carrick, J. D., & Cooperstock, F. I. 2012, *Ap&SS*, **337**, 321
Casertano, S. 1983, *MNRAS*, **203**, 735
Ciotti, L. 2021, *Introduction to Stellar Dynamics* (Cambridge: Cambridge Univ. Press) (C21)
Ciotti, L., & Pellegrini, S. 1996, *MNRAS*, **279**, 240
Clark, S. J., & Tucker, R. W. 2000, arXiv:gr-qc/0003115v2
Cooperstock, F. I., & Tieu, S. 2007, *IJMPA*, **22**, 2293
Costa, L. F. O., & Natário, J. 2021, *Univ*, **7**, 388
Cross, D. J. 2006, arXiv:astro-ph/0601191v1
Crosta, M., Giammaria, M., Lattanzi, M., & Poggio, E. 2020, *MNRAS*, **496**, 2107
Deledicque, V. 2019, arXiv:1903.10061
Feynman, R. P., Leighton, R. B., & Sands, M. 1977, *The Feynman Lectures on Physics*, Vol. 2 (Reading, MA: Addison-Wesley)
Fitzpatrick, R. 2012, *An Introduction to Celestial Mechanics* (Cambridge: Cambridge Univ. Press)
Fuchs, B., & Phleps, S. 2006, arXiv:astro-ph/0604022v1
Gradshteyn, I. S., Ryzhik, I. M., Jeffrey, A., & Zwillinger, D. 2007, *Table of Integrals, Series, and Products* (7th ed.; New York: Elsevier) (GR07)
Griffiths, D. J. 1999, *Introduction to Electrodynamics* (Englewood Cliffs, NJ: Prentice-Hall)
Hunter, C. 1977, *AJ*, **82**, 271
Jackson, D. 1998, *Classical Electrodynamics* (3rd ed.; New York: Wiley), J98
Kalnajs, A. J. 1983, in *IAU Symp. 100, Internal Kinematics of Galaxies*, ed. E. Athanassoula (Dordrecht: Reidel), 87
Kent, S. M. 1986, *AJ*, **91**, 1301
Korzynski, M. 2005, arXiv:astro-ph/0508377v2
Kuzmin, J. G. 1956, *Astron. Zh*, **33**, 27
Landau, L. D., & Lifshitz, E. M. 1971, *The Classical Theory of Fields* (Oxford: Pergamon Press)
Ludwig, G. O. 2021, *EPJC*, **81**, 186
Ludwig, G. O. 2022, *EPJC*, **82**, 281
Lynden-Bell, D., & Nouri-Zonoz, M. 1998, *RvMP*, **70**, 427
Mashhoon, B. 2008, arXiv:gr-qc/0311:030

- Mashhoon, B., Gronwald, F., & Lichtenegger, I. M. 1999, arXiv:gr-qc/9912027v1
Mathai, A. M., Saxena, R. K., & Haubold, H. J. 2010, *The H-Function* (Berlin: Springer)
Miyamoto, M., & Nagai, R. 1975, *PASJ*, **27**, 533
Nagai, R., & Miyamoto, M. 1976, *PASJ*, **28**, 1
Ostriker, J. P., & Peebles, P. J. E. 1973, *ApJ*, **186**, 467
Panofsky, W. K. H., & Phillips, M. 1962, *Classical Electricity and Magnetism* (2nd ed.; Reading, MA: Addison-Wesley)

- Poisson, E., & Will, C. M. 2014, *Gravity* (Cambridge: Cambridge Univ. Press)
- Prudnikov, A. P., Brychkov, Yu. A., & Marichev, O. I. 1986, *Integrals and Series*, Vol. 2 (Philadelphia, PA: Gordon & Breach) (P86)
- Prudnikov, A. P., Brychkov, Yu. A., & Marichev, O. I. 1990, *Integrals and Series*, Vol. 3 (Philadelphia, PA: Gordon & Breach)
- Rindler, W. 1997, *PhLA*, [233](#), [25](#)
- Rowland, D. R. 2015, *IJMPD*, [24](#), [1550065](#)
- Ruggiero, M. L. 2002, arXiv:[gr-qc/0207065v2](#)
- Ruggiero, M. L. 2021, *Univ*, [7](#), [451](#)
- Ruggiero, M. L., Ortolan, A., & Speake, C. C. 2021, arXiv:[2112.08290v1](#)
- Satoh, C. 1980, *PASJ*, [32](#), [41](#)
- Smet, C. O., Posacki, S., & Ciotti, L. 2015, *MNRAS*, [448](#), [2921](#)
- Toomre, A. 1963, *ApJ*, [138](#), [385](#)
- Toth, V. T. 2021, *IJMPD*, [30](#), [2150102](#)
- van Albada, T. S., Bahcall, J. N., Begeman, K., & Sancisi, R. 1985, *ApJ*, [295](#), [305](#)
- van Albada, T. S., & Sancisi, R. 1986, *RSPTA*, [320](#), [447](#)
- Vogt, D., & Letelier, P. S. 2005a, arXiv:[astro-ph/0510750v1](#)
- Vogt, D., & Letelier, P. S. 2005b, arXiv:[astro-ph/0512553v1](#)